Kovove Mater. 52 2014 107–112
DOI: 10.4149/km_2014_2_107

Boriding kinetics of pure cobalt

A. Çalik[1], M. S. Karakaş[1], N. Uçar[2]*, F. Ünüvar[1]

[1] *Suleyman Demirel University, Faculty of Technology, Manufacturing Engineering Department, 32260 Isparta, Turkey*
[2] *Suleyman Demirel University, Faculty of Science and Arts, Physics Department, 32260 Isparta, Turkey*

Received 26 September 2013, received in revised form 4 December 2013, accepted 12 December 2013

Abstract

Kinetics of boride layers and hardness of pure cobalt (Co) have been investigated. Powder pack boriding method was carried out at 1173 and 1273 K for 1, 3 and 6 h. X-ray diffraction analysis of boride layers on the surface of pure Co revealed the existence of CoB and Co_2B phases. The growth rate constant and activation energy for the boride layer were determined. The obtained results show that although the boride layer thickness increases with the increasing boriding temperature and time, these parameters have no significant effect on the hardness of the boride layer or the matrix. A decrease in the value of hardness moving from the boride layer to main structure was observed. In addition, the obtained hardness values on the boride layer at some boride parameters show a hardness anomaly due to structural defects or different type of the borides.

Key words: boronizing, powder pack, boride kinetics, activation energy, hardness

1. Introduction

Cobalt is a hard ferromagnetic metal with properties similar to iron. It is used industrially in a number of ways such as in the preparation of magnetic, wear resistant and creep resistant alloys [1–3]. Coating with certain compounds is one way of improving material properties such as hardness, wear performance and corrosion resistance [4, 5]. One of the coating techniques is boriding (also known as boronizing), a thermo-chemical surface hardening process in which boron atoms are diffused into the surface of the work piece to form complex borides (e.g., FeB/Fe_2B in iron) with the base metal [6–8]. Pack boriding is the most commonly used boriding method. In this method the specimen to be borided is usually "packed" in a steel container with a powder containing the boriding agent, SiC, which is used as a diluent, and KBF_4, which acts as an activator [9–11]. It has been successfully applied to various ferrous and nonferrous metals. Pack boriding of transition metals has shown limited success; in some metals (e.g., nickel) the presence of SiC and KBF_4 in the boriding powder results in the formation of silicides and borosilicides which generally have a negative influence on the hardness of the boride layer [12–16]. In the present study, pure cobalt was borided using the powder pack method using commercial Ekabor III powders containing SiC and KBF_4. Characterization of the borided specimens was carried out by optical microscopy, X-ray diffraction, and microhardness measurements. In addition, growth kinetics for the boride layers was studied by measuring the thickness of the boride layer as a function of time in the temperature range of 1173–1273 K.

2. Experimental method

Commercial purity specimens of Co were cut with the dimensions of 2 mm × 40 mm × 5 mm. The boriding of the pure Co specimens was achieved in a solid medium using the powder pack method. In this method, the specimens were thoroughly mixed with commercial Ekabor-III powders to form the boriding pack. The pack was heat treated in an electrical resistance furnace for exposure times of 1, 3 and 6 h at 1173 and 1273 K under atmospheric pressure. After this process, borided specimens were removed from the furnace and cooled in air. Borided specimens were sectioned from one side and prepared metallographic-

---

*Corresponding author: e-mail address: nazmucar@yahoo.com ally up to 1200-grid emery paper and then polished using 0.3 μm alumina pastes. Polished samples were etched with 4% Nital before examination.

Microstructure analysis of borides formed on the pure Co samples was performed with optical microscope (Olympus-PMEU) and a JEOL JSM-6400 model scanning electron microscope (SEM). The presence of borides on the surface of the borided pure cobalt was determined by using the X-ray diffractometer (Rigaku D-MAX 2200) at 40 kV and 20 mA, with Cu Kα radiation of 0.15418 nm wavelength, over a 2θ range from 20° to 100 ℃. The thickness of boride layer was measured by means of a digital thickness measuring instrument attached to an optical microscope. The distance between the outer surface of the boride layer and the tip of the boride pins was measured at different locations and an average value for layer thickness was found. To determine the hardness of the borided pure cobalt a Vickers microhardness tester with a load of 100 g was used. Many indentations were made on each coating film under each experimental condition to check the reproducibility of hardness data.

3. Results and discussion

3.1. Microstructure characterization and layer thickness

SEM micrographs of the borided pure Co specimens at 1173 and 1273 K for 1, 3 and 6 h are given in Figs. 1, 2.

At higher magnifications, two distinct regions were identified in the cross-sections of the borided pure Co surfaces; the boride layer and the matrix unaffected by boron. A transition zone which is usually observed in many steels was absent. On the other hand, as can be seen from these photographs, the boride layers on formed borided Co specimens have a needle-shaped structure, similar to that observed in iron. In addition, from Fig. 3 it is observed that CoB and Co_2B phases formed on the surface of the boride layer when pure Co was borided at 1173 K for 1 h. At increased boriding times and temperatures, only one phase, CoB, was detected in the boride layer due to enhanced boron diffusion (Fig. 3a,b).

Mu et al. [16] observed that Co_2B, Co_2B+Co_2Si and Co_2Si phases form on the surface of borided with commercial LSBII powders (that contain SiC) for pure Co samples borided for 8 h at 1123, 1173 and 1223 K, respectively. From the same study, X-ray peaks for the borides could not be observed when pure Co was borided at 1223 K for 8 h due to the silicide phase covering the boride layer. This result was explained by the low penetration depth of X-rays for cobalt silicide; hence the borides beneath the silicide phase could be detected. In this study, the boriding temperature of 1273 K and the boron potential were high enough for the formation of the CoB phase. At 1173 K, Co_2B was the predominant phase in the boride layer due to the decreased diffusion rate of boron. Trace amounts of CoB were detected in the specimen borided at 1173 K for 1 h. However, increasing the boronizing time at 1173 K resulted in the transformation of the CoB phases to Co_2B. Similar transformations from

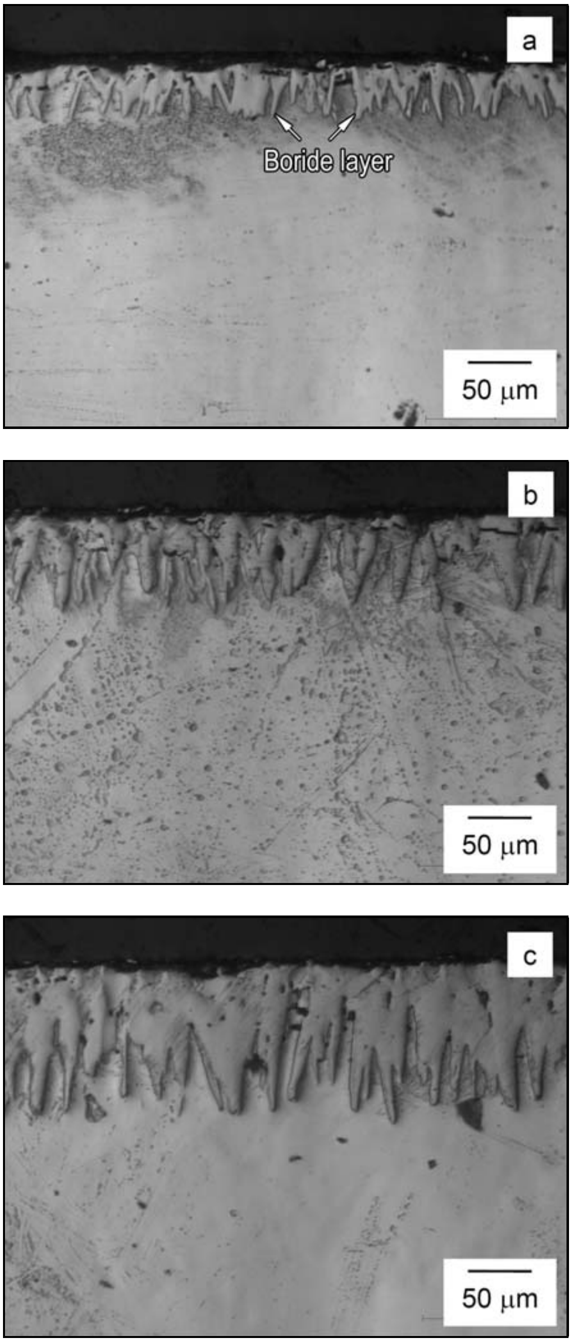

Fig. 1. SEM cross-section view of borided pure Co samples at (a) 1, (b) 3 and (c) 6 h for 1173 K.

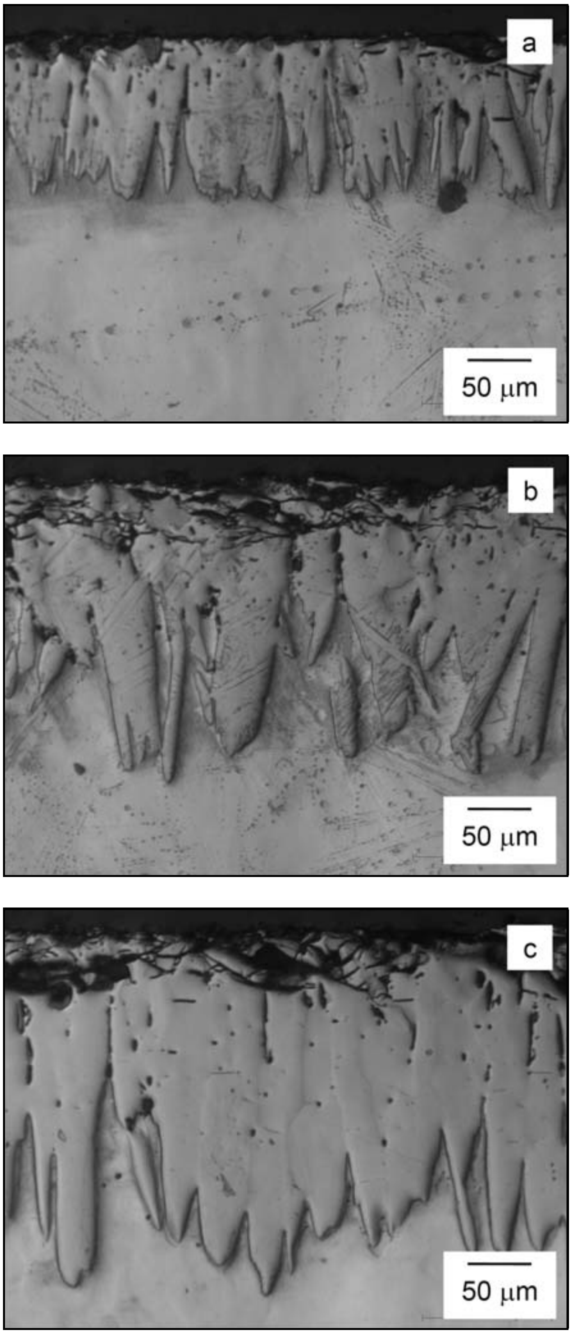

Fig. 2. SEM cross-section view of borided pure Co samples at (a) 1, (b) 3 and (c) 6 h for 1273 K.

FeB to Fe_2B have been observed by Dybkov [17] during high temperature annealing in borided FeCr alloys in the absence of the boriding mixture. While three cobalt borides (Co_3B, Co_2B and CoB) are possible according to the Co-B phase diagram, only Co_2B and CoB phases were observed in this study. The reason for this is the high boron potential of the boriding medium; lower boron potentials (and possibly lower temperatures) could have favored the formation of the Co_3B phase.

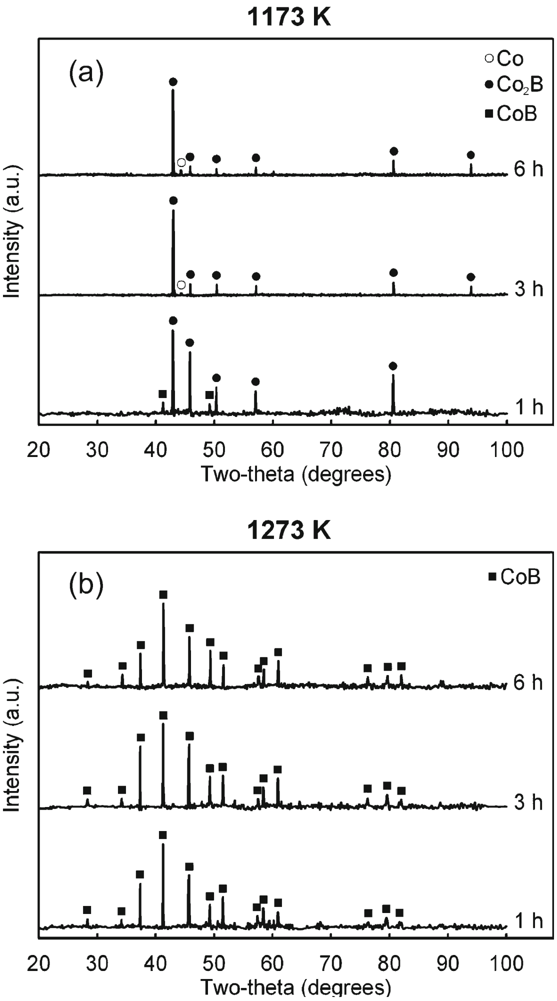

Fig. 3. XRD patterns of borided pure Co samples at (a) 1173 K and (b) 1273 K.

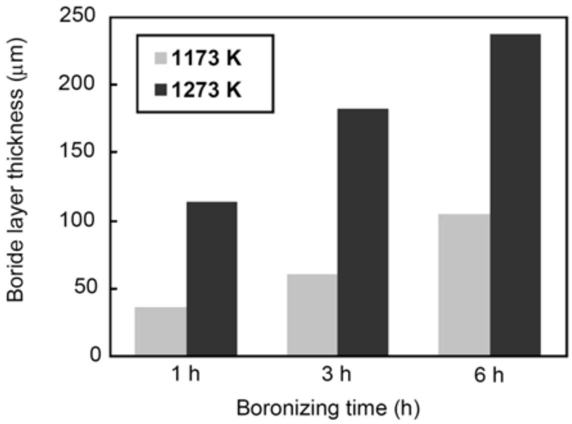

Fig. 4. Boride layer thickness vs. boriding time, showing the increase in boride layer thickness with increasing time and temperature.

Figure 4 shows a graphical representation of the variation of a boride layer thickness with boriding

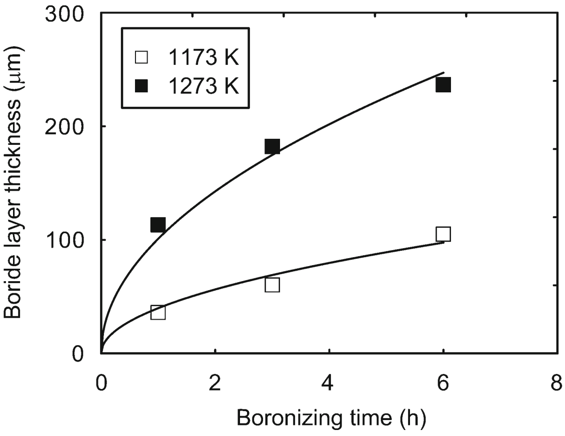

Fig. 5. Variation of the boride layer thickness as a function of boriding time.

temperature and time obtained from optical and SEM photographs; it was observed that the thickness of the boride layer increases with increasing temperature and time. In the literature [18–20], it has been pointed out that the thickness of a boride layer depends strongly on the boriding time, the chemical composition of the material to be borided, the process temperature, and the techniques used, such as gas, liquid and pack boriding. For borided pure Co samples, it can be said that the boride layer thickness increases when the boriding temperature and time are increased due to the increased diffusion of boron atoms from the boriding mixture into the substrate. Although the obtained results on boride layer thickness are the same as those of pure Ni borided with commercial LSB-II powder at 1123–1223 K for 2–8 h [21], these values are fairly higher than those of pure Nb, W and Cr [22] due to crystal structure. It is well known that diffusivity of boron atoms is different in each metal according to crystal structure.

3.2. Boride kinetics

It is well known that kinetic parameters such as processing temperature and time must be known for the control of boriding treatment. The main factor limiting the growth of layer is the diffusion of boron into the substrate. From thickness data obtained from the borided layer, the growth rate constant for boron can be calculated for each temperature with the following equation:

$$d^2 = Kt, \tag{1}$$

where d is the thickness of boride layer (mm), t is the boriding time (s), and K is the growth rate constant with respect to boriding temperature. As can be seen from Fig. 5, the boride layer thickness is parabolically increasing with time. This indicates that layer growth kinetics obeys a parabolic law due to diffusion--controlled process. The obtained results are in agreement with the results taken from the literature [23–27]. Corresponding to this, Keddam [27] suggested a mathematical model based on Fick's laws to simulate the growth kinetics of boride layer on the iron substrate under certain assumptions. This diffusion model was able to estimate the thickness of boride layers and predict the boron-depth – concentration profiles for boride phases as a function of time, temperature and boron surface concentration. On the other hand, growth rate constant can be derived from the slope of boride layer thickness and square root of time by means of Eq. (1). In the present study, the obtained effective growth rate constants with respect to boriding temperature 1173 and 1273 K are $0.44 \times 10^{-8}\ \mathrm{cm^2\,s^{-1}}$ and $2.83 \times 10^{-8}\ \mathrm{cm^2\,s^{-1}}$ for borided pure Co samples, respectively. This result indicates that growth rate constant increases with increasing boriding temperature. On the other hand, the obtained growth rate constant is higher than that of steels due to alloy elements. In literature, it has been pointed out that the growth rate constant also changes with the carbon content in steels, which confirms that growth rate of boride layer controlled by boron diffusion decreases with increasing carbon content [24, 28, 29].

It is possible to argue that the relationship between growth rate constant K, activation energy Q, and the temperature T (K), can be expressed by the Arrhenius equation:

$$K = K_0 \exp\left(\frac{-Q}{RT}\right), \tag{2}$$

where K_0 is a pre-exponential constant, Q is the activation energy for boron diffusion ($\mathrm{J\,mol^{-1}}$), T is the absolute temperature in (K) and R is the universal gas constant ($\mathrm{J\,mol^{-1}\,K^{-1}}$). Consequently, the activation energy Q for boron diffusion in the boride layer is determined by the slope obtained by the plot ln K vs. $1/T$ using Eq. (2). In this study, the calculated activation energy for the formation of the boride layer on the surface of the pure Co specimens was $231.7\ \mathrm{kJ\,mol^{-1}}$. In literature, it has been pointed that the boron activation energy depends upon the C content in steels and also the other alloy elements. Corresponding to this, the activation energies of AISI 52100, AISI 440C steels and pure Fe have been obtained as $269.638\ \mathrm{kJ\,mol^{-1}}$, $340\ \mathrm{kJ\,mol^{-1}}$ [26] and $90\ \mathrm{kJ\,mol^{-1}}$ [30], respectively, for pack boriding. These results show that activation energy of borided samples is different from each other due to crystal structure, strength of atomic bonding and purity of the samples.

3.3. Microhardness

Figure 6 shows the microhardness profile measured

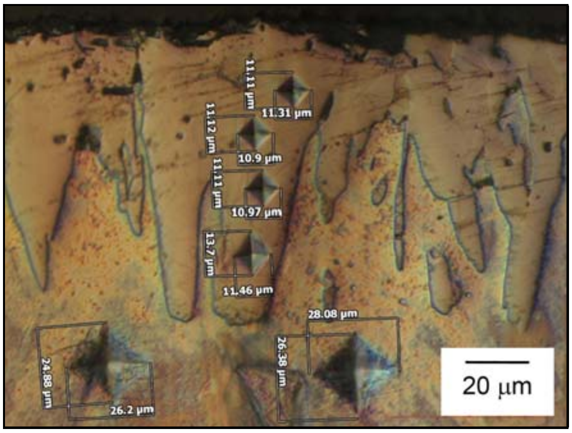

Fig. 6. View of Vickers indentations from the outer layer to the interior of the base material in a borided pure Co, 1173 K for 3 h.

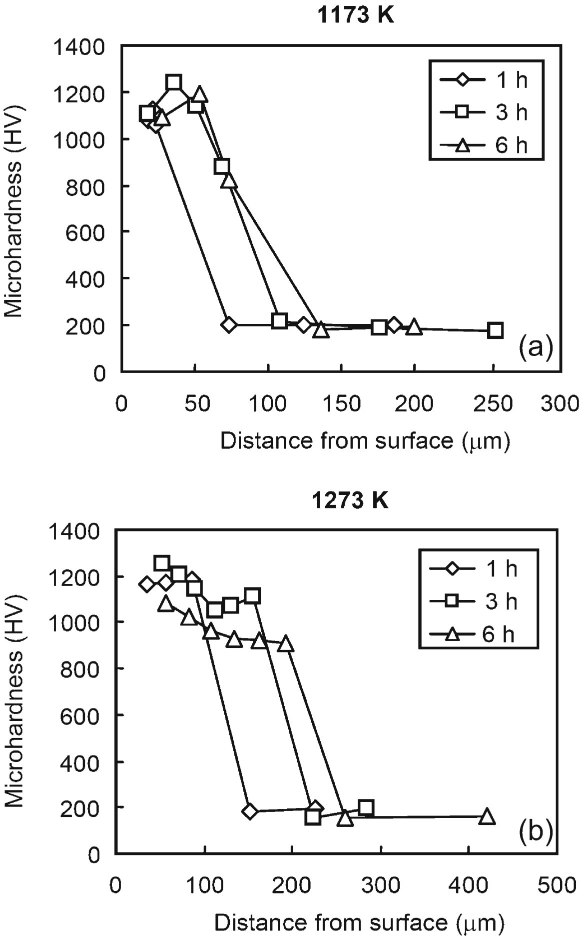

Fig. 7. Microhardness vs. distance from the surface to the interior of the base materials for a borided pure Co, (a) 1173 K and (b) 1273 K.

on the cross section of the pure Co borided at 1173 K for 3 h under atmospheric pressure.

Figure 7 shows the variation of hardness of pure Co with respect to the different boriding time for 1173 and 1273 K, respectively.

As can be seen in these figures, hardness of boride layer is much higher than that of matrix due to hard boride CoB and Co_2B phases. The high hardness of the surface is mainly a result of the presence of boride layers, but is additionally due to solid solution hardening between Co and boron atoms in the matrix. Summarizing, after the boriding treatment at 1173 and 1273 K, the surface hardness was increased by a factor close to 6 in comparison with the matrix. In contrast to this, although the boride layer thickness increases with increasing boriding temperature and time, these boriding parameters had no significant effect on the boride layer hardness of pure Co samples in the present study (Fig. 7a,b). In the literature [31–34], it has been shown that both boride layer thickness and hardness increase with increasing boriding temperature and time. On the other hand, the obtained hardness behaviour on the boride layer at boriding time 3 h, 6 h for 1173 K and 1 h for 1273 K showed hardness anomaly. The known surface improvement results show that with increasing distance from surface to matrix, the hardness decreases continuously as obtained borided 1 h for 1173 K and 3, 6 h for 1273 K. We think that the fluctuated hardness in the boride layer of some borided pure Co samples, hardness anomaly, may be due to structural defects such as porosity and cracks on the surface or formed different boron phases [35].

4. Conclusions

The results of the current study can be summarized as follows:

– A thick borided layer with a needle-shaped structure identified as CoB and Co_2B formed on the surface of borided pure Co specimens.

– It was observed that the boride layer thickness increased with increasing treating temperature. These boride parameters have no significant effect on the hardness of pure Co specimens.

– The obtained hardness behavior on the boride layer at some boride parameters shows a hardness anomaly due to structural defects or different type of the borides.

– The activation energy for borided pure Co samples was 231.7 kJ mol^{-1}, which is much lower than that for many borided steels.

References

[1] Enghag, P.: Cobalt. Encyclopedia of the Elements: Technical Data – History – Processing – Applications.

Weinheim, Wiley-VCH 2004. doi:10.1002/9783527612338.ch30

[2] Shedd, K. B.: Mineral Year book 2006: Cobalt. Reston, United States Geological Survey 2006.

[3] Cobalt Facts. Wickford, Essex, The Cobalt Development Institute 1996.

[4] Atik, E.: Mater. Struct., *31*, 1998, p. 418. doi:10.1007/BF02480716

[5] Mann, B. S.: Wear, *208*, 1997, p. 125. doi:10.1016/S0043-1648(96)07374-7

[6] Arun, S., Sivakumar, T., Viswanathan, P., Subramanian, R.: Int. J. of Eng. Res. and Appl., *3*, 2013, p. 1927.

[7] Sinha, A. K.: Boriding (Boronizing) of Steels. ASM Handbook, Heat Treating, vol. 4. Materials Park, ASM International 2002.

[8] Lee, S. Y., Kim, G. S., Kim, B.-S.: Surf. Coat. Technol., *177*, 2004 p. 178. doi:10.1016/j.surfcoat.2003.07.009

[9] Yu, L. G., Chen, X. J., Khor, K. A., Sundararajan, G.: Acta Mater., *53*, 2005, p. 2361. doi:10.1016/j.actamat.2005.01.043

[10] Gunes, I., Kayali, Y., Ulu, S.: Indian J. of Eng. and Mater. Sci., *19*, 2012, p. 397.

[11] Novak, P., Filip, V., Michalcova, A.: In: Proceeding of 21st International Conference on Metallurgy and Materials. Ostrava, ANGER Ltd. 2012, p. 908, ISBN 978-80-87294-31-4.

[12] Vangaveti, R.: Boron induced surface modification of transition metals. [M.Sc. Thesis]. New Jersey, New Jersey Institute of Technology 2006.

[13] Mu, D., Shen, B., Yang, C., Zhao, X.: Vacuum, *83*, 2009, p. 1481. doi:10.1016/j.vacuum.2009.06.048

[14] Usta, M., Ozbek, I., Ipek, M., Bindal, C., Ucisik, A. H.: Surf. Coat. Technol., *194*, 2005, p. 330. doi:10.1016/j.surfcoat.2004.06.042

[15] Usta, M., Ozbek, I., Bindal, C., Ucisik, A. H., Ingole, S., Liang, H.: Vacuum, *80*, 2006, p. 1321. doi:10.1016/j.vacuum.2006.01.036

[16] Mu, D., Yang, C., Shen, B. I., Jiang, H.: J. Alloys Comp., *479*, 2009, p. 629. doi:10.1016/j.jallcom.2009.01.015

[17] Dybkov, V. I.: J. Mater. Sci., *42*, 2007, p. 6614. doi:10.1007/s10853-007-1512-2

[18] Knotek, O., Lungsheider, E., Leuschen, K.: Thin Solid Films, *45*, 1977, p. 331. doi:10.1016/0040-6090(77)90266-8

[19] Kemih, H., Sasaki, C., Kitamura, M., Satomi, N., Ueda, Y., Nishikawa, M.: J. Nuclear Mater., *26*, 1999, p. 1108. doi:10.1016/S0022-3115(98)00856-3

[20] Ozbek, I., Bindal, C.: Surf. Coat. Technol., *154*, 2002, p. 14. doi:10.1016/S0257-8972(01)01409-8

[21] Mu, D., Shen, B.-L., Yang, C., Zhao, X.: Vacuum, *83*, 2009, p. 1481. doi:10.1016/j.vacuum.2009.06.048

[22] Usta, M., Ozbek, I., Bindal, C., Ucisik, A. H., Ingoled, S., Liang, H.: Vacuum, *80*, 2006, p. 1321. doi:10.1016/j.vacuum.2006.01.036

[23] Taguchi, O., Tiwara, G. P., Iijiwa, Y.: Mater. Trans., *44*, 2003, p. 1. doi:10.2320/matertrans.44.83

[24] Milinovic, A., Krumes, D., Markovic, R.: Technical Bulletin, *19*, 2012, p. 1.

[25] Hannech, E. B., Lamoudi, N., Gasmi, A.: Surf. Rev. Lett., *11*, 2004, p. 337. doi:10.1142/S0218625X04006232

[26] Kayali, Y., Gunes, I., Ulu, S.: Vacuum, *86*, 2012, p. 14. doi:10.1016/j.vacuum.2012.03.030

[27] Keddam, M.: Appl. Surf. Sci., *236*, 2004, p. 451. doi:10.1016/j.apsusc.2004.05.141

[28] Fellner, P., Chrenkova, M.: Chem. Papers, *46*, 1992, p. 226.

[29] Nur Hafizah Abd Aziz, Iswadi Jauhari, Hanis Ayuni Mohd Yusof, Nor Wahida Ahamad: In: Proceeding of 3rd International Conference on Integrity, Reliability and Failure. Eds.: Gomes, S. J. F., Meguid, S. A. Porto, Portugal, INEGI Editions 2009, paper ref: S2414_P0226.

[30] Asthana, P., Liang, H., Usta, M., Ucisik, A. H.: J. Tribol., *129*, 2007, p. 1. doi:10.1115/1.2401211

[31] Li, C., Shen, B., Li, G., Yang C.: Sur. Coat. Tech., *202*, 2008, p. 5882. doi:10.1016/j.surfcoat.2008.06.170

[32] Ucar, N., Aytar, O., Calik, A.: Mater. Technol., *46*, 2012, p. 6.

[33] Gunes, I.: J. Mater. Sci. Technol., *29*, 2013, p. 7. doi:10.1016/j.jmst.2013.04.005

[34] Yan, P. X., Zhang, X. M., Xu, J. W., Wu, Z. G., Song, Q. M.: Mater. Chem. Phys., *71*, 2001, p. 107. doi:10.1016/S0254-0584(01)00270-X

[35] Gunduz, K. O., Gencer, Y., Tarakci, M., Calik, A.: Sur. Coat. Tech., *221*, 2013, p. 104. doi:10.1016/j.surfcoat.2013.01.034